

# SPECTRAL INSTABILITY FOR SOME SCHRÖDINGER OPERATORS

A. ASLANYAN AND E. B. DAVIES

September 1998

ABSTRACT. We define the concept of instability index of an isolated eigenvalue of a non-self-adjoint operator, and prove some of its general properties. We also describe a stable procedure for computing this index for Schrödinger operators in one dimension, and apply it to the complex resonances of a typical operator with a dilation analytic potential.

*AMS subject classification:* 34L05, 35P05, 47A75, 49R99, 65L15

*Keywords:* Eigenvalue, Spectral Instability, Computational Spectral Theory, Schrödinger Operator, Non-Self-Adjoint, Pseudospectrum, Complex Resonance, Dilation Analyticity

## 1. INTRODUCTION

In some earlier papers we showed that typical non-self-adjoint Schrödinger operators  $H$  exhibit spectral instability in the following sense. For any  $\varepsilon > 0$  there exist many  $\lambda \in C$  and  $f \in Dom(H)$  such that

$$\|Hf - \lambda f\|_2 \leq \varepsilon \|f\|_2$$

even though  $\lambda$  is not near the spectrum of  $H$ . This behaviour occurs for the harmonic oscillator with a nonreal coupling constant as well as for many non-self-adjoint anharmonic oscillators. There is a rapidly growing literature on pseudospectral theory, which was invented to explore just such possibilities, [5, 6, 8, 9, 10, 15, 16, 17, 18, 19, 20].

---

The authors thank the Engineering and Physical Sciences Research Council for support under grant No. GR/L75443

In this paper we return to the same type of operator, but measure spectral instability by a method which provides more precise information about the instability of individual eigenvalues. We have computed the so-called instability indices of the first 100 eigenvalues  $\lambda_n$  of the harmonic oscillator, and see that they appear to increase exponentially with  $n$ . We have carried out a similar but more limited exercise for the resonances of a typical Schrödinger operator with dilation analytic potential, and report our conclusions.

Our definition of the instability index of an isolated eigenvalue  $\lambda$  of  $H$  of multiplicity 1 involves the fact that the eigenfunction  $f$  of  $H$  associated with  $\lambda$  is different from the eigenfunction  $f^*$  of  $H^*$  associated with its eigenvalue  $\bar{\lambda}$ . In Section 2 we show that the instability index

$$\kappa(\lambda) := \frac{\|f\|_2 \|f^*\|_2}{|\langle f, f^* \rangle|}$$

of  $\lambda$  is equal to the norm of the spectral projection  $P$  associated with  $\lambda$ , and also present a number of other theoretical properties of the index.

If  $H := -\Delta + V$  acts in  $L^2(\mathbb{R}^N)$  where  $V$  is a complex-valued potential then  $H^* = -\Delta + \bar{V}$  and  $f^* = \bar{f}$ . Hence for any isolated eigenvalue we have

$$(1) \quad \kappa(\lambda) = \frac{\int_{\mathbb{R}^N} |f|^2}{|\int_{\mathbb{R}^N} f^2|}.$$

Note that when  $\kappa(\lambda)$  is large the eigenvalue is very unstable under small perturbations of the potential, and hence also unstable because of rounding errors in the computation. The numerical task we face is to compute the eigenvalue and the instability index accurately in situations in which the denominator of (1) is very small because the complex-valued eigenfunction  $f$  is oscillating rapidly.

Because the spectral instability develops so rapidly as  $n$  increases, we have had to take great care to use computational methods which are reliable. Fortunately for our first problem there are independent methods of checking the values which we have obtained. In the second case we use the experience gained by the first problem, and have checked the reliability of the conclusions under the variation of several different parameters in the computational method. In Section 6 we summarize the conclusions of our investigation.

## 2. THE INSTABILITY INDEX

If  $\lambda$  is an isolated point of the spectrum of a closed operator  $A$  in a Hilbert space  $\mathcal{H}$ , the spectral projection  $P$  associated with  $\lambda$  is defined by

$$P\phi := \frac{1}{2\pi i} \int_{\gamma} (z - A)^{-1} \phi dz$$

where  $\gamma$  is any sufficiently small closed contour winding around  $\lambda$ . The assumption that this projection has rank 1 is stronger than the assumption that  $\lambda$  is an eigenvalue of multiplicity 1.

**Lemma 1.** *If  $f$  and  $f^*$  are the normalised eigenvectors of  $A$  and  $A^*$  associated with the eigenvalues  $\lambda$  and  $\bar{\lambda}$  respectively, and if  $P$  has rank 1, then  $\langle f, f^* \rangle \neq 0$  and the instability index of  $\lambda$  is equal to  $\|P\|$ .*

Proof We have

$$\begin{aligned} \text{Ker}(P) &= (\text{Ran}(P^*))^{\perp} \\ &= \{g : \langle g, f^* \rangle = 0\}. \end{aligned}$$

Since  $f \notin \text{Ker}(P)$  we see that  $\langle f, f^* \rangle \neq 0$ . It is now easy to verify that  $P$  is given by

$$Ph := \frac{\langle h, f^* \rangle}{\langle f, f^* \rangle} f$$

and hence that

$$\|P\| = \frac{1}{|\langle f, f^* \rangle|} = \kappa(\lambda).$$

**Theorem 1.** *If  $P$  has rank 1 then*

$$\kappa(\lambda) = \sup\{a_1(V) : \|V\| \leq 1\}$$

where  $a_1(V)$  is defined to be the coefficient of  $s$  in the expansion of the eigenvalue of the perturbed operator  $H + sV$ :

$$\lambda(s) = \lambda + a_1(V)s + a_2(V)s^2 + \dots$$

Proof By standard arguments in perturbation theory [14] we have

$$(H + sV)(f + sg + \dots) = (\lambda + s\mu + \dots)(f + sg + \dots)$$

where the perturbed eigenvector is normalised by

$$\langle f + sg + \dots, f^* \rangle = \langle f, f^* \rangle.$$

We deduce that  $Hg + Vf = \lambda g + \mu f$  and  $\langle g, f^* \rangle = 0$ . Therefore

$$\langle Hg, f^* \rangle + \langle Vf, f^* \rangle = \mu \langle f, f^* \rangle$$

and

$$\mu = \frac{\langle Vf, f^* \rangle}{\langle f, f^* \rangle}.$$

The proof is completed by the observation that

$$\sup\{|\langle Vf, f^* \rangle| : \|V\| \leq 1\} = \|f\| \|f^*\|.$$

The instability index is also related to the notion of pseudospectrum, which is a geometric way of looking at resolvent norm properties. Namely if  $\varepsilon > 0$  we put

$$Spec_\varepsilon(A) := \{z \in C : \|(z - A)^{-1}\| > \varepsilon^{-1}\}.$$

The sizes of these sets, which all contain the spectrum of  $A$ , measure the spectral instability of  $A$ . One always has

$$\{z : \text{dist}\{z, Spec(A)\} < \varepsilon\} \subseteq Spec_\varepsilon(A)$$

but the RHS is often much larger than the LHS. The following theorem states that if  $\kappa(\lambda)$  is large then the component of  $Spec_\varepsilon(A)$  containing  $\lambda$  is large in a related sense. Several similar results can be obtained in the same manner.

**Theorem 2.** *Suppose that the spectral projection  $P$  associated with the isolated eigenvalue  $\lambda$  of  $A$  has rank 1. Let  $\gamma$  be a closed contour surrounding the connected component of  $Spec_\varepsilon(A)$  which contains  $\lambda$  but does not intersect  $Spec_\varepsilon(A)$ . Then*

$$|\gamma| \geq 2\pi\varepsilon\kappa(\lambda)$$

where  $|\gamma|$  is the length of  $\gamma$ .

Proof We have

$$\kappa(\lambda) = \|P\| = \left\| \frac{1}{2\pi i} \int_\gamma \frac{dz}{z - A} \right\| \leq \frac{1}{2\pi\varepsilon} \int_\gamma |dz| = \frac{|\gamma|}{2\pi\varepsilon}.$$

## 3. THE COMPUTATIONAL PROCEDURES

**3.1. Finding Eigenvalues.** Let  $H$  be the Schrödinger operator

$$(2) \quad Hf(x) := -\frac{d^2f}{dx^2} + V(x)f(x)$$

acting in  $L^2(\mathbb{R})$ . Let us first outline briefly the method for determining the eigenvalues of  $H$ . For any  $z \notin [0, \infty)$  there exist two solutions  $f_{\pm}$  of

$$(3) \quad Hf = zf$$

which vanish as  $x \rightarrow \pm\infty$  respectively. We introduce *transfer functions*  $g_{\pm} := f'_{\pm}/f_{\pm}$  satisfying nonlinear first order differential equations to be given below and proper initial conditions at  $\pm\infty$ . We wish to solve the Cauchy problem for  $g_{-}(x)$  for  $x \geq X_{-}$  and for  $g_{+}(x)$  for  $x \leq X_{+}$  where  $X_{-} < 0$ ,  $X_{+} > 0$ ,  $|X_{-}|$  and  $X_{+}$  are sufficiently large. Provided we know initial conditions for  $g_{\pm}$  at  $X_{\pm}$  which correspond to  $f_{\pm}$  vanishing at  $\pm\infty$  respectively, the two Cauchy problems can be solved by a standard numerical method. The question how to transfer the so-called admissible boundary conditions from singular points (which are  $\pm\infty$  in our case) has been extensively studied by A. A. Abramov and his collaborators (a survey of their results can be found in [2]). Naturally, the behaviour of the potential  $V$  has to be taken into account: say, if  $V$  is bounded and vanishes rapidly at infinity then  $g_{\pm}$  are asymptotically constant as  $x \rightarrow \pm\infty$ , respectively. Later on in this section we shall consider this and other cases applying the ideas of [2].

To locate the eigenvalues in terms of the transfer functions we choose  $a \in \mathbb{R}$  and consider

$$F(z) = F(z; a) := g_{+}(a) - g_{-}(a).$$

This function is meromorphic on  $\mathbb{C} \setminus [0, \infty)$  with zeros at the eigenvalues of the operator  $H$ . The zeros are independent of  $a$  but  $F$  may also have poles which depend on  $a$ . They are at the eigenvalues of the restrictions of  $H$  to  $L^2(a, \infty)$  and  $L^2(-\infty, a)$  subject to Dirichlet boundary conditions at  $a$  in both cases.

To determine the zeros of  $F$  numerically we use the argument principle (cf. [3] for a contour integration procedure) to obtain their approximate positions followed by some variant of Newton's method to obtain accurate values. One has to be careful not to choose a value of  $a$  for which there is a pole close to the zero of interest, so it is recommended that a few different values of  $a$  are investigated.

The numerical elaboration of the above ideas involves a substantial amount of preliminary work. One may find the approximate location of the eigenvalues and of the maxima of the eigenfunctions by an independent method. For example if one

discretises a large enough interval in the real line then one can find approximate eigenvalues by a standard matrix eigenvalue routine; MATLAB is ideal for this purpose. Another possibility is to use JWKB asymptotic formulae which also enable one to find an interval  $(X_-, X_+)$  outside which the relevant eigenfunction is negligible, and a point  $x_0$  at which the modulus of the eigenfunction takes its maximum value (see the next subsection in this regard).

If the potential  $V$  is an even function with respect to reflection about the origin, then every eigenfunction is either even or odd, and the problem may be decomposed into two independent problems on  $[0, \infty)$ , with Dirichlet or Neumann boundary conditions at 0. This is the case in our examples. From now on in this subsection we concentrate on the symmetric problem and take advantage of symmetry. Actual computational formulae are given below for the case of the half-line. Note that the theory of admissible boundary conditions based upon asymptotic analysis of solutions of the differential equation at  $\pm\infty$  applies in a generic situation.

Auxiliary Cauchy problems to be solved numerically are as follows. Let us first assume that  $V(x) \sim cx^2$ ,  $x \rightarrow \infty$ , where  $c \in \mathbb{C}$  is constant — this corresponds to the harmonic oscillator problem and its perturbations studied in the next section. For a fixed value of  $z$  we consider the solution  $f_+$  of (3) vanishing as  $x \rightarrow \infty$  and introduce a new transfer function  $\alpha_+$  satisfying

$$\frac{1}{x}\alpha'_+ + \sqrt{c}\alpha_+^2 + \frac{1}{x^2\sqrt{c}}(\sqrt{c}\alpha_+ - V + z) = 0, \quad \alpha_+(X) \sim -1 + O\left(\frac{1}{X^2}\right), \quad X \rightarrow \infty$$

where  $X$  is sufficiently large. According to [2],

$$f'_+(x)/f_+(x) = \sqrt{cx}\alpha_+(x)$$

for such  $x \geq 0$  that  $\alpha_+(x)$  exists. Moreover, one can work out the coefficients of the asymptotic expansion of  $\alpha_+$  for a particular potential  $V(x)$ . For  $V(x) = cx^2$ , say, we replace the condition at infinity by

$$\alpha_+(X) = -1 + \frac{d}{X^2} + \frac{\sqrt{cd^2 - d}}{2\sqrt{c}X^4}, \quad d = \frac{z - \sqrt{c}}{2c},$$

choosing  $X$  so that the last term in the above formula is negligible. Along the lines of the mentioned paper we pose the so-called admissible condition at infinity for the considered potential. The above initial condition is equivalent to the boundary condition  $f_+ \rightarrow 0$  at infinity, up to terms of order  $O(\frac{1}{X^6})$  as  $X \rightarrow \infty$ .

Next, we are going to consider the operator  $H$  with a potential vanishing rapidly

enough at infinity (see Section 5). Following the same approach, we introduce

$$g_+(x) = f'_+(x)/f_+(x), \quad x \geq 0,$$

and for this function obtain the singular Cauchy problem

$$g'_+ + g_+^2 - V + z = 0, \quad g_+(x) \sim i\sqrt{z}, \quad x \rightarrow \infty.$$

Clearly, the initial conditions vary for different types of potential. Still, for each particular choice of  $V$  we are able to apply the developed theory and set appropriate initial conditions for transfer equations. After that has been done we integrate those equations numerically from  $X$  from right to left to some (fixed)  $a \geq 0$ . The transfer functions  $\alpha_+$ ,  $g_+$  actually take their values in the Riemann sphere, so we have to switch between them and their inverses at certain values of  $x$ . As soon as  $|\alpha_+|$  or  $|g_+|$  becomes greater than a prescribed constant we change to  $\alpha_+^{-1}$  or  $g_+^{-1}$ , respectively and from this point on integrate analogous equations starting with proper initial conditions for the inverse functions. After a finite number of changes of this kind we reach the chosen point  $a$ .

To complete the transfer procedure, consider the solution  $f_0$  of (3) satisfying  $f'_0(0) = 0$ . We denote

$$f'_0(x)/f_0(x) = g_0(x)$$

and solve

$$g'_0 + g_0^2 - V(x) + z = 0, \quad g_0(0) = 0$$

from left to right. (Obvious changes should be made when considering an odd solution  $f_0$  satisfying a Dirichlet boundary condition at  $x = 0$ .) Again, we switch from  $g_0$  to  $g_0^{-1}$  if necessary and stop at the same point  $a$ .

Remark that the described procedure is the simplest version of the boundary condition transfer, or pivotal condensation method we have chosen for the second order equation. There is an extensive literature (cf. [1, 4, 11] etc.) on the transfer methods where much more advanced techniques are developed. Although there are other possibilities, in this paper we get satisfactory results implementing the above version.

Finally, we have  $g_0$  (corresponding to either odd or even  $f_0$ ) and  $g_+$  calculated at the same point  $a$ . If

$$F(\lambda; a) := g_+(a) - g_0(a) = 0$$

then  $\lambda$  is an eigenvalue of  $H$ . Thus, we evaluate  $F(z; a)$  for certain values of  $z$  as described and then find the eigenvalues of interest as zeros of  $F(z; a)$ . As has already been mentioned, we first use the argument principle (see [3] for computational formulae) to locate the eigenvalues and then apply an iterative Newton-like

method to obtain more precise values. After an eigenvalue has been located up to the required accuracy, one can compute the corresponding eigenfunction by recovering its values from the transfer functions  $g_+$ ,  $g_0$ .

The method proposed has been implemented as a universal Fortran 77 code including all the basic procedures described above in this section. Auxiliary Cauchy problems have been solved by a standard routine based on the Runge–Kutta–Merson fourth order method. In our computations we have used 32-bit and 64-bit arithmetic.

The question remains how to choose  $a$  — although the zeros of  $F(z; a)$  do not depend on  $a$ , in practical computations the choice of  $a$  does play a significant role. In fact, we investigated different functions  $F(z; a)$  for a wide range of  $a$ . One of the possible choices is  $a = 0$ . For problems with even potentials the zeros and the poles of  $F(z; a)$  interchange (see Figures 1a, 1b, 2a). We use contour map plots to find initial guesses for eigenvalues when there is no other a-priori information about their location. Plotting contour maps with the use of Matlab 5.2 has also helped us to avoid poles when looking for zeros. Thus, in a generic situation we recommend that one calculates the values of  $F(z)$  (for which we have used our Fortran code), then produces the plots (Matlab graphics) and, finally, finds eigenvalues accurately (a standard iterative Fortran procedure).

We regard our numerical results obtained via the above method as reliable. In particular, this is confirmed by several values of  $a$  providing entirely different functions  $F(z)$  whose zeros coincide. These results are to be reported below in the following two sections.

**3.2. Calculating the Instability Index.** The second stage in the process is to compute the instability index defined by (1). The obvious method, namely calculating the two integrals after first determining the eigenfunction numerically, is highly inaccurate if the instability index is large. The reason is that the integrand in the denominator is highly oscillatory, and the evaluation of such integrals is problematical. The following method is much superior in applications. Below we present a technique suitable for an arbitrary (not necessarily symmetric) potential.

We introduce four functions as follows. For  $x \in [a, X_+]$  we define

$$h_+(x) := f(x)^{-2} \int_x^{X_+} f(s)^2 ds$$

$$k_+(x) := |f(x)|^{-2} \int_x^{X_+} |f(s)|^2 ds$$

where  $f$  is the eigenfunction associated with the eigenvalue  $\lambda$ . Similarly for  $x \in [X_-, a]$  we define

$$\begin{aligned} h_-(x) &:= f(x)^{-2} \int_{X_-}^x f(s)^2 ds \\ k_-(x) &:= |f(x)|^{-2} \int_{X_-}^x |f(s)|^2 ds. \end{aligned}$$

It is obvious that

$$\frac{k_-(a) + k_+(a)}{|h_-(a) + h_+(a)|} = \frac{\int_{X_-}^{X_+} |f(x)|^2 dx}{\left| \int_{X_-}^{X_+} f(x)^2 dx \right|}$$

which converges exponentially rapidly to  $\kappa$  as  $X_+ \rightarrow +\infty$  and  $X_- \rightarrow -\infty$ . The task is to find a procedure to evaluate the four functions accurately. We consider only  $h_-$ , the others being similar. It follows from its definition that  $h_-(X_-) = 0$  and that  $h_-$  satisfies the differential equation

$$(4) \quad h_-(x)' = 1 - 2g_-(x)h_-(x).$$

This may be solved numerically, say, by a Runge-Kutta method to determine  $h_-(a)$ .

It is important to be sure that the solutions of (4) and the other three equations are stable. It suffices to note that  $\text{Re } g_+(X_+) < 0$  and  $\text{Re } g_-(X_-) > 0$ , which implies the stability of the solutions  $h_+$ ,  $k_+$  and  $h_-$ ,  $k_-$  from right to left and from left to right, respectively. This has been confirmed by numerical tests. The same is true for the transfer equations quoted in the previous subsection — the solution  $\alpha_+$ , for instance, is known to be stable from right to left which is essential for practical computations.

There is a potential problem in that if  $f(b) = 0$  for some  $b \in (X_-, a)$  then  $h_-$  is usually infinite at that point. Generically one does not expect a complex-valued  $C^2$  function of a real variable to vanish anywhere, and we have not seen this problem arise, but one needs to discuss how the method should be adapted in the event of its occurrence. There are two cases, which are distinguished numerically by whether  $h_-(x) \rightarrow 0$  as  $x \rightarrow b$  or  $|h_-(x)| \rightarrow \infty$  as  $x \rightarrow b$ . Note that since  $f$  is a non-zero solution of (3) and  $f(b) = 0$  it follows that  $f'(b) \neq 0$ , so  $|g(x)| \rightarrow \infty$  as  $x \rightarrow b$ .

**Lemma 2.** *If  $f(b) = 0$  and  $\int_{X_-}^b f(s)^2 ds = 0$  then  $h_-(x) \rightarrow 0$  as  $x \rightarrow b$  and  $g(x)h_-(x) \rightarrow 1/3$  as  $x \rightarrow b$ .*

Proof Neglecting lower order terms we have

$$\begin{aligned} h_-(x) &\sim (x-b)/3 \\ g(x) &\sim (x-b)^{-1} \end{aligned}$$

as  $x \rightarrow b$ . The results follow.

Thus, in this case we are still able to integrate the same equation (4); the point  $b$  is, in fact, regular rather than singular.

The more standard case is that in which  $f(b) = 0$  and  $\int_{X_-}^b f(s)^2 ds \neq 0$ . Clearly  $|h_-(x)| \rightarrow \infty$  as  $x \rightarrow b$ .

**Lemma 3.** *If we put  $\tilde{h}_-(x) := h_-(x)^{-1}$  then  $\tilde{h}_-(x) \rightarrow 0$  and  $\tilde{h}_-(x)g(x) \rightarrow 0$  as  $x \rightarrow b$  and*

$$(5) \quad \tilde{h}_-(x)' = \tilde{h}_-(x)^2 - 2\tilde{h}_-(x)g(x)$$

for all  $x$  near  $b$ .

Proof Neglecting lower order terms we have

$$\begin{aligned} \tilde{h}_-(x) &\sim \frac{f'(b)^2(x-b)^2}{\int_{X_-}^b f(s)^2 ds} \\ \tilde{h}_-(x)g(x) &\sim \frac{f'(b)^2(x-b)}{\int_{X_-}^b f(s)^2 ds} \end{aligned}$$

as  $x \rightarrow b$ . The verification that  $\tilde{h}_-(x)$  satisfies the differential equation (5) is routine.

Thus, in the considered case we recommend to change to  $\tilde{h}$  at  $x = b$  and integrate (5) instead of (4).

Naturally, the stability of the procedure proposed in this subsection depends heavily on  $a$  (though the exact value of  $\kappa$  does not depend on the norm of  $f$ ). A proper choice of  $a$  is very important and can essentially influence the results. Choosing  $a = \operatorname{argmax}|f(x)|$  seems to be a reasonable way.

Compared to standard approaches the above mentioned technique has two clear advantages. First, we do not need to evaluate the fast oscillating integrands  $f(x)^2$  and  $|f(x)|^2$  themselves — instead, we integrate several auxiliary ODEs. Secondly, this procedure is numerically stable. In the cases which we have examined the solutions  $h_{\pm}$ ,  $k_{\pm}$  change quite slowly and smoothly.

**3.3. Possible Difficulties.** If the instability index of an eigenvalue is very large then it is clear from Theorem 2 that the eigenvalue is intrinsically difficult to compute. One mechanism by which this can occur in computations is that at the eigenvalues, for which one knows that  $F(\lambda) = 0$ , one also finds that  $F'(\lambda)$  is very small, so it is not possible to locate  $\lambda$  accurately. The following theorem provides a link in one direction between these two phenomena at a theoretical level.

We assume that

$$Hf(x) := -\frac{d^2f}{dx^2} + V(x)f(x)$$

on  $L^2(R)$ , where  $V(x)$  vanishes rapidly enough as  $|x| \rightarrow \infty$ . Given  $a \in R$  and  $z \in C$  satisfying  $\operatorname{Re}(i\sqrt{z}) < 0$ , let  $g_+(z, x)$  be the solution of

$$g'(x) + g(x)^2 + z - V(x) = 0$$

on  $[a, \infty)$  subject to  $g_+(z, x) \sim i\sqrt{z}$  as  $x \rightarrow \infty$ . Let  $g_-(z, x)$  be the solution of the same equation on  $(-\infty, a]$  subject to  $g_-(z, x) \sim -i\sqrt{z}$  as  $x \rightarrow -\infty$ . We put

$$F(z) = g_+(z, a) - g_-(z, a)$$

as usual so that  $F(\lambda) = 0$  if and only if  $\lambda$  is an eigenvalue of  $H$ .

**Theorem 3.** *Let  $\kappa(\lambda)$  be the instability index at an eigenvalue  $\lambda$ , let  $f$  be the associated eigenfunction and assume that  $g := f'/f$  is bounded on  $R$ . Then*

$$\kappa(\lambda)|F'(\lambda)| \|g\|_\infty \geq 1.$$

Proof If  $\varepsilon > 0$  is small enough there exists

$$\mu = \lambda + \frac{\varepsilon}{F'(\lambda)} + O(\varepsilon^2)$$

such that  $F(\mu) = \varepsilon$ . Now put

$$\begin{aligned} \tilde{g}_-(x) &:= g_-(\mu, x) + \varepsilon/2 \\ \tilde{g}_+(x) &:= g_+(\mu, x) - \varepsilon/2 \end{aligned}$$

for the appropriate values of  $x$ , so that

$$\tilde{g}_+(a) - \tilde{g}_-(a) = 0.$$

We have

$$\begin{aligned} \tilde{g}'_-(x) &= \tilde{V}(x) - \mu - \tilde{g}_-(x)^2 \\ \tilde{g}'_+(x) &= \tilde{V}(x) - \mu - \tilde{g}_+(x)^2 \end{aligned}$$

under the following conditions on  $\tilde{V}$ . If  $x > a$  then

$$\begin{aligned}\tilde{V}(x) - V(x) &= \tilde{g}'_+(x) + \mu + \tilde{g}_+(x)^2 - V(x) \\ &= g_+(\mu, x)' + \mu + (g_+(\mu, x) - \varepsilon/2)^2 - V(x) \\ &= -\varepsilon g_+(\mu, x) + \varepsilon^2/4\end{aligned}$$

while if  $x < a$  we must have

$$\begin{aligned}\tilde{V}(x) - V(x) &= \tilde{g}'_-(x) + \mu + \tilde{g}_-(x)^2 - V(x) \\ &= g_-(\mu, x)' + \mu + (g_-(\mu, x) + \varepsilon/2)^2 - V(x) \\ &= \varepsilon g_-(\mu, x) + \varepsilon^2/4\end{aligned}$$

Therefore

$$\|\tilde{V} - V\|_\infty = \sup\{\varepsilon\|g_+(\mu, \cdot)\|_\infty + O(\varepsilon^2), \varepsilon\|g_-(\mu, \cdot)\|_\infty + O(\varepsilon^2)\}.$$

But  $g_\pm(\mu, x) \rightarrow g(x)$  uniformly as  $\mu \rightarrow \lambda$  by the assumptions of this section, so

$$\|\tilde{V} - V\|_\infty = \varepsilon\|g\|_\infty + o(\varepsilon).$$

The statement of the theorem now follows from the formula for the instability index given in Theorem 2.

In the two examples considered below,  $F'(z)$  is very small for large values of  $|z|$ , so it is impossible to determine its zeros. This seems to be the main barrier to the determination of large eigenvalues.

#### 4. THE HARMONIC OSCILLATOR

**4.1. Basic Facts.** Consider the operator  $H$  defined by (2) with the potential  $V(x) = cx^2$ , referred to as  $H_o$  in the rest of the paper. The eigenvalue problem for  $H_o$  is called the *harmonic oscillator* problem and is known to have infinitely many eigenvalues  $\lambda_n^{(o)} = \sqrt{c}(2n + 1)$ ,  $n = 0, 1, \dots$ . The corresponding eigenfunctions  $f_n = C_n e^{-\sqrt{c}x^2/2} \phi_n(\sqrt[4]{c}x)$  where  $C_n$  are normalising constants,  $\phi_n$  denote Hermite polynomials,  $Re \sqrt{c} > 0$ . These eigenfunctions are either even or odd:  $f_{2k}(x) = f_{2k}(-x)$ ,  $f_{2k+1}(x) = -f_{2k+1}(-x)$ ,  $k = 0, 1, \dots$ . As proposed in Section 3, we consider  $H_o$  on the half-line adding either Neumann or Dirichlet boundary conditions at the origin. We have used it as a sample problem to check the above method for finding eigenvalues and eigenfunctions. Indeed, the results thus obtained are in very good accordance with the theory; they confirm the reliability of the method. It allowed us to calculate  $\sim 100$  eigenvalues of  $H_o$  up to the accuracy  $\delta \in (10^{-10}, 10^{-4})$ .

When implementing the method of Section 3 we found that the accurate numerical determination of the eigenvalue  $\lambda_n$  for  $n > 100$  is not possible using double precision (64-bit) arithmetic, particularly because  $F'(z)$  can be very small near the points where  $F(z) = 0$ . We computed the instability indices for the first 100 eigenvalues, using the JWKB approximation to the eigenfunction  $f_n$  associated with the eigenvalue  $\lambda_n^{(o)}$  as described in [9, 10]. This approximation suggests that  $|f_n(x)|$  takes its maximum near  $x = a_n$  and

$$f_n(a_n + y) = e^{-i\eta_n y + O(y^2)}$$

where the real constants  $a_n$  and  $\eta_n$  are computed from

$$\sqrt{c}(2n + 1) = \eta_n^2 + ca_n^2.$$

Having an appropriate value of  $a_n$  is, of course, helpful when we calculate  $\kappa_n$  by means of the method given in Subsection 3.2.

**4.2. Perturbations of the Operator  $H_o$ .** Let us present some results concerned a perturbation of the harmonic oscillator operator

$$H_W := H_o + W(x).$$

We have investigated various perturbations of the form  $W(x) = \varepsilon e^{imx}$  for a range of fairly small  $\varepsilon$ . The reason is that looking for the perturbation providing the most unstable results, one has to choose  $W(x)$  as follows. From the perturbation theory formula cited in the proof of Theorem 1 one can easily see that among perturbations satisfying

$$|W(x)| \leq \varepsilon$$

the function

$$W_n(x) = \varepsilon \frac{\bar{f}_n(x)}{f_n(x)}$$

provides the worst perturbation of the  $n$ -th eigenvalue of  $H_o$ . Indeed we then have

$$(6) \quad \lambda_n = \lambda_n^{(o)} + \varepsilon \kappa(\lambda_n^{(o)}) + o(\varepsilon).$$

If we only take account of the first term of the JWKB expansion for  $f_n$ , we obtain the perturbing potential

$$\tilde{W}_n(x) = \varepsilon e^{2i\eta_n x}$$

after removing an irrelevant phase factor. The expectation that  $\tilde{W}_n$  provides a perturbation of the eigenvalue almost as great as that due to  $W_n$  is tested below. We tabulate below the absolute values of the corrections to several eigenvalues  $\lambda_n$  of  $H_W$  calculated numerically by means of the method described in Section 3.

Tables 1–3 contain the values of  $|\lambda_n^{(o)} - \lambda_n|$  for  $c = \sqrt{i}$  and  $W(x) = \varepsilon e^{imx}$ . The figures related to  $\varepsilon = 0$  give the absolute errors of the computation of the  $n$ -th eigenvalue of  $H_o$ .

Table 1. Values of  $|\lambda_n^{(o)} - \lambda_n|$ ,  $n = 9$ ,  $2\eta_n = 6.4133$ 

$\varepsilon \backslash m$	1.0	5.0	6.0	6.4133	7.0	10.0
0	$10^{-10}$					
$10^{-6}$	$7.9 \cdot 10^{-7}$	$6.6 \cdot 10^{-6}$	$7.7 \cdot 10^{-6}$	$8.0 \cdot 10^{-6}$	$7.8 \cdot 10^{-6}$	$2.9 \cdot 10^{-7}$
$10^{-5}$	$8.6 \cdot 10^{-6}$	$6.4 \cdot 10^{-5}$	$7.9 \cdot 10^{-5}$	$8.1 \cdot 10^{-5}$	$7.7 \cdot 10^{-5}$	$1.9 \cdot 10^{-6}$
$10^{-4}$	$8.7 \cdot 10^{-5}$	$6.4 \cdot 10^{-4}$	$8.0 \cdot 10^{-4}$	$8.0 \cdot 10^{-4}$	$7.7 \cdot 10^{-5}$	$1.8 \cdot 10^{-5}$
$10^{-3}$	$8.7 \cdot 10^{-4}$	$6.42 \cdot 10^{-3}$	$7.97 \cdot 10^{-3}$	$8.16 \cdot 10^{-3}$	$7.66 \cdot 10^{-3}$	$1.7 \cdot 10^{-4}$

Table 2. Values of  $|\lambda_n^{(o)} - \lambda_n|$ ,  $n = 19$ ,  $2\eta_n = 9.1884$ 

$\varepsilon \backslash m$	5.0	9.0	9.1884	10.0	20.0
0	$10^{-8}$				
$10^{-8}$	$1.0 \cdot 10^{-7}$	$4.0 \cdot 10^{-6}$	$3.9 \cdot 10^{-6}$	$1.1 \cdot 10^{-6}$	$6.1 \cdot 10^{-7}$
$10^{-7}$	$2.6 \cdot 10^{-6}$	$3.25 \cdot 10^{-5}$	$3.22 \cdot 10^{-5}$	$2.63 \cdot 10^{-5}$	$6.2 \cdot 10^{-7}$
$10^{-6}$	$3.7 \cdot 10^{-5}$	$3.25 \cdot 10^{-4}$	$3.20 \cdot 10^{-4}$	$2.77 \cdot 10^{-4}$	$6.1 \cdot 10^{-7}$
$10^{-5}$	$4.0 \cdot 10^{-4}$	$3.20 \cdot 10^{-3}$	$3.20 \cdot 10^{-3}$	$2.80 \cdot 10^{-3}$	$6.3 \cdot 10^{-7}$

Table 3. Values of  $|\lambda_n^{(o)} - \lambda_n|$ ,  $n = 29$ ,  $2\eta_n = 11.3014$ 

$\varepsilon \backslash m$	10.0	11.0	11.3014	12.0	20.0
0	$10^{-6}$				
$10^{-10}$	$2 \cdot 10^{-6}$	$2 \cdot 10^{-6}$	$3 \cdot 10^{-6}$	$3 \cdot 10^{-6}$	$10^{-6}$
$10^{-9}$	$1.2 \cdot 10^{-5}$	$1.5 \cdot 10^{-5}$	$1.4 \cdot 10^{-5}$	$1.4 \cdot 10^{-5}$	$10^{-6}$
$10^{-8}$	$1.14 \cdot 10^{-4}$	$1.48 \cdot 10^{-4}$	$1.46 \cdot 10^{-4}$	$1.34 \cdot 10^{-4}$	$10^{-6}$
$10^{-7}$	$1.141 \cdot 10^{-3}$	$1.454 \cdot 10^{-3}$	$1.441 \cdot 10^{-3}$	$1.336 \cdot 10^{-3}$	$10^{-6}$
$10^{-6}$	0.01142	0.01455	0.01453	0.01334	$10^{-6}$
$10^{-5}$	0.11657	0.14927	0.14563	0.13670	$10^{-6}$

First of all, the above results show that the values of  $|\lambda_n^{(o)} - \lambda_n|$  are approximately proportional to  $\varepsilon$ , that is, confirm formula (6) numerically. In fact, for very small  $\varepsilon$  the method can only feel the first order corrections to the eigenvalues of the harmonic oscillator within the chosen accuracy as expected. Secondly, maximal perturbations of eigenvalues are observed for  $m \approx 2\eta_n$  which justifies the above arguments.

**4.3. Another Approach. Instability Index.** We have also investigated the harmonic oscillator using the quantum mechanical creation and annihilation operators  $A^*$  and  $A$ . This is not possible for generic differential operators, but provides a method of testing the general algorithms developed in the last section. In this language

$$\begin{aligned} H_o &= P^2 + cQ^2 \\ &= -(A^* - A)^2/2 + c(A^* + A)^2/2 \\ &= (c - 1)A^{*2}/2 + (c + 1)A^*A + (c - 1)A^2/2 + (c + 1)/2. \end{aligned}$$

If  $\{\phi_n\}_{n=0}^\infty$  is the orthonormal basis of Hermite functions in  $\mathcal{H} := L^2(\mathbb{R})$ , then  $A\phi_n = \sqrt{n}\phi_{n-1}$  and  $A^*\phi_n = \sqrt{n+1}\phi_{n+1}$  for all  $n$ , and we may represent  $H_o$  by means of the infinite matrix

$$H_{o,m,n} := \begin{cases} a_m & \text{if } m = n \\ b_m & \text{if } n = m + 2 \\ b_n & \text{if } m = n + 2 \\ 0 & \text{otherwise} \end{cases}$$

with respect to this basis, where  $m, n = 0, 1, 2, \dots$  and

$$\begin{aligned} a_m &:= (c + 1)(m + 1/2) \\ b_m &:= (c - 1)\{(m + 1)(m + 2)\}^{1/2}/2. \end{aligned}$$

The even and odd subspaces  $\mathcal{H}_0$  and  $\mathcal{H}_1$  with respect to reflection about 0 are invariant under  $H_o$ , and these subspaces may also be characterised by

$$\begin{aligned} \mathcal{H}_0 &= \text{lin}\{\phi_{2n} : n = 0, 1, \dots\} \\ \mathcal{H}_1 &= \text{lin}\{\phi_{2n+1} : n = 0, 1, \dots\}. \end{aligned}$$

Restricting the matrix to either of these subspaces renders it tri-diagonal, so numerical computations are particularly easy and accurate. We compute the instability index of an eigenvalue  $\lambda_r = \sqrt{c}(2r + 1)$  for  $r = 0, 1, \dots$  by evaluating

$$\kappa_r := \frac{\sum_{n=0}^{N-1} |f(n)|^2}{|\sum_{n=0}^{N-1} f(n)^2|}$$

where  $f$  is the eigenvector associated with  $\lambda_r$ , obtained by solving the obvious recurrence relation starting from  $n = 0$ . Note that  $\lambda_r$  is taken to be an exact eigenvalue of the infinite matrix, not an eigenvalue of the truncated  $N \times N$  matrix. For a particular eigenvalue  $\lambda_r$ ,  $N$  must be large enough for the coefficients  $f_n$  with  $n > N$  to be insignificant, but not so large that the recurrence relation

becomes unstable. For  $r > 50$  it is not possible to satisfy both of these conditions simultaneously using standard double precision 32-bit arithmetic, and we used the high precision arithmetic of Maple V.4.

The delicacy of the computations is indicated by the evaluation of  $\kappa_{100} \sim 2.5594 \times 10^{16}$  for  $c = \sqrt{i}$ . For  $N = 200$  this required us to use the command ‘*Digits = 30*’ in Maple V.4, but putting  $N = 500$ , we only obtained the same result for ‘*Digits = 110*’ or greater. The instability in the solution of the recurrence relation is evidently more important than the contributions of the terms of the series in the range  $200 < n < 500$ . The following results (see Table 4) were all obtained with  $N = 200$  and ‘*Digits = 100*’, and appear to be reliable.

The instability indices tabulated below have been obtained in two independent ways. The methods developed in this and the previous sections turned out to provide very close results for the first 40 eigenvalues. This can be seen from Table 4 where  $\kappa_n^{(1)}$  is related to the method of this section, and  $\kappa_n^{(2)}$  to that of Section 3. The figures obtained for  $n \geq 40$  are clearly different for the two methods although they are qualitatively of the same order.

Table 4. Instability indices of  $H_o$ ,  $c = \sqrt{i}$

$n$	0	10	20	30	40	50
$\kappa_n^{(1)}$	1.0404	14.2777	563.2146	$2.5789 \cdot 10^4$	$1.2625 \cdot 10^6$	$6.3627 \cdot 10^7$
$\kappa_n^{(2)}$	1.0404	14.2777	563.2146	$2.5789 \cdot 10^4$	$1.2625 \cdot 10^6$	$6.3649 \cdot 10^7$
$n$	60	70	80	90	100	
$\kappa_n^{(1)}$	$3.2734 \cdot 10^9$	$1.7081 \cdot 10^{11}$	$9.0059 \cdot 10^{12}$	$4.7860 \cdot 10^{14}$	$2.5594 \cdot 10^{16}$	
$\kappa_n^{(2)}$	$3.2922 \cdot 10^9$	$1.7110 \cdot 10^{11}$	$8.9063 \cdot 10^{12}$	$4.0052 \cdot 10^{14}$	$1.9261 \cdot 10^{16}$	

The growth of the instability index corresponds to the values of  $|\lambda_n^{(o)} - \lambda_n|$  increasing with  $n$  (see also Tables 1–3). Results to be cited below provide another numerical evidence of this fact. In Table 5 the values of  $|\lambda_n^{(o)} - \lambda_n|$ ,  $c = \sqrt{i}$ , corresponding to the perturbing potentials  $\tilde{W}_n$  are given. Comparing Table 5 to Table 4 we conclude that  $\mu_n \approx \kappa_n$  which indicates reasonably good agreement of our numerical results and perturbation theory.

Table 5. Values of  $|\lambda_n^{(o)} - \lambda_n|$ ,  $\tilde{W}_n(x) = \varepsilon e^{2i\eta_n x}$ ,  $c = \sqrt{i}$

$\varepsilon \setminus n$	30	40	50	60
$10^{-6}$	0.021542	1.19860		
$10^{-7}$	0.002155	0.10747		
$10^{-8}$	0.000216	0.01056	0.54950	
$10^{-9}$	$2.2 \cdot 10^{-5}$	0.00105	0.05518	2.4921
$10^{-10}$	$3 \cdot 10^{-6}$	0.00010	0.00587	0.2587
$10^{-11}$		$10^{-5}$	0.00059	0.0279
$10^{-12}$			$6 \cdot 10^{-5}$	0.0028
0	$10^{-6}$	$5 \cdot 10^{-6}$	$10^{-5}$	$10^{-4}$

Analysing the rate of divergence of the instability index of  $H_o$  in Table 4, one can notice that it grows exponentially:  $\kappa_n \sim e^{0.4n}$  for the studied range of  $n$ .

The eigenfunctions for the harmonic operator with nonreal coupling constant do not form an unconditional basis, [9]. If they formed a conditional basis the projections  $P_n$  associated with the eigenvalues  $\lambda_n = \sqrt{c}(2n+1)$  as in Lemma 1 would be uniformly bounded in norm by a standard argument, [12]. However, we have obtained strong numerical evidence that the norms increase exponentially with  $n$ . We therefore make the conjecture that for nonreal coupling constant the eigenfunctions of the harmonic oscillator do not form a conditional basis.

More precisely let  $N > 0$  and let  $P_N$  be the spectral projection of  $H_o$  associated with the first  $N$  complex eigenvalues  $\lambda_n^{(o)}$  where they are ordered in increasing absolute values. Explicitly

$$P_N f := \sum_{n=0}^{N-1} \frac{\langle f, f_n^* \rangle}{\langle f_n, f_n^* \rangle} f_n.$$

If  $\|P_N f - f\| \rightarrow 0$  as  $N \rightarrow +\infty$  for all  $f \in \mathcal{H}$  then the uniform boundedness theorem implies that there exists a constant  $C$  such that  $\|P_N\| \leq C$  for all  $N$ . From the inequality

$$\|P_N - P_{N-1}\| \leq 2C$$

we are then able to deduce that the instability index  $\kappa_n$  is a bounded function of  $n$ . This conflicts with the numerical evidence that these indices increase exponentially with  $n$ . We have attempted to confirm the exponential increase by using the JWKB approximations to the eigenfunctions constructed in [9, 10], but the eigenfunctions oscillate so rapidly for high eigenvalues that the JWKB approximations were not useful. While we have not proved the exponential increase of  $\kappa_n$  the corresponding result for the pseudospectrum (resolvent norms) has been proved in [10] not just for the harmonic oscillator but for a wide range of anharmonic oscillators.

## 5. COMPLEX RESONANCES

**5.1. Definitions.** Let  $H$  be the Schrödinger operator

$$\hat{H}f(x) := -\frac{d^2f}{dx^2} + V(x)f(x)$$

acting in  $L^2([0, \infty))$  subject to Dirichlet or Neumann boundary conditions at  $x = 0$ , where the potential  $V$  is bounded and vanishes at infinity. For any positive constant  $c$  we define

$$\begin{aligned} \hat{H}_c f(x) &:= \left( D_c \hat{H} D_{c^{-1}} f \right) (x) \\ (7) \qquad &= -c^{-2} \frac{d^2 f}{dx^2} + V(cx) f(x) \end{aligned}$$

where  $D_c$  is the unitary dilation operator

$$D_c f(x) := \sqrt{c} f(cx).$$

We observe that  $\hat{H}_c$  is unitarily equivalent to  $\hat{H}$ . If  $V$  is an entire function on  $C$  then the formula (7) defines a family of non-self-adjoint operators parametrised by  $c \in C$ ,  $c \neq 0$ . Under suitable conditions the eigenvalues of these operators are known to be independent of  $c$ , and are called *resonances* of  $\hat{H}$ ; see [7, 13] for expositions of the theory of dilation analytic resonances. Since the operators  $\hat{H}_c$  are unitarily equivalent for values of  $c$  with the same argument, we only consider  $c$  of the form  $c := e^{i\theta/2}$  where  $0 < \theta < \pi/2$ .

We investigate the particular case of the operator

$$H_0 f(x) := -\frac{d^2 f}{dx^2} + x^2 e^{-x^2/b^2} f(x)$$

where  $b > 0$  is to be fixed. If one imposes a Dirichlet boundary condition at  $x = 0$ , this operator determines the evolution in the zero angular momentum sector of a three-dimensional quantum particle trapped by a rotationally invariant barrier, where the particle may tunnel through the barrier and escape to infinity. Because the potential is non-negative and vanishes rapidly at infinity,  $H_0$  has absolutely continuous spectrum  $[0, \infty)$  and no eigenvalues. A direct calculation shows that

$$H_\theta f(x) := \hat{H}_{e^{i\theta/2}} f(x) = -e^{-i\theta} \frac{d^2 f}{dx^2} + e^{i\theta} x^2 e^{-e^{i\theta} x^2/b^2} f(x).$$

We consider  $H_\theta$  subject to either Dirichlet or Neumann boundary conditions at  $x = 0$ . The potential of this operator vanishes rapidly as  $x \rightarrow \infty$  provided  $0 < \theta < \pi/2$ . Under this condition  $H_\theta$  has essential spectrum  $e^{-i\theta} \times [0, \infty)$  and also some

isolated eigenvalues in the sector  $\{z : -\theta < \arg z \leq 0\}$ , these being independent of  $\theta$ .

For large values of  $b$  (we take  $b = 100$ ) the potential of  $H_\theta$  is similar to that of the complex harmonic oscillator, and the eigenvalues of  $H_\theta$  are close to the values  $\{2n + 1 : n = 0, 1, \dots\}$ . For smaller values of  $b$  there are several resonances very close to the positive real axis, but at a certain point they turn sharply away into the lower half plane.

**5.2. Location of Resonances.** The reason for there being resonances very close to the real axis is as follows. Let us consider the operator  $H_\theta$  as a perturbation of the harmonic oscillator operator  $H_o$ . In our notation we now have

$$H_\theta = H_o + W(t, \nu), \quad W(t, \nu) = t^2(e^{-t^2/b^2} - 1)$$

where we put  $t = e^{i\theta/2}x$  and  $\nu = 1/b^2$ . Regarding  $\nu$  as a small parameter we expand

$$W(t, \nu) = \sum_{k=1}^{\infty} W_k(t) \nu^k = \sum_{k=1}^{\infty} \frac{(-1)^k t^{2(k+1)}}{k!} \nu^k.$$

Again, for an arbitrary  $n$ , following the standard perturbation theory approach, we expand the  $n$ -th eigenvalue of  $H_\theta$  as

$$(8) \quad \lambda_n(\nu) \sim \lambda_n^{(o)} + \sum_{k=1}^{\infty} \mu_k \nu^k$$

which is a non-convergent asymptotic expansion, and calculate

$$(9) \quad \mu_1 = \frac{\int_{-\infty}^{\infty} W_1(t) f_n^2 dt}{\int_{-\infty}^{\infty} f_n^2 dt} = -C_n^2 \int_{-\infty}^{\infty} t^4 e^{-t^2} \phi_n^2(t) dt.$$

Here we follow the notations of Section 4:  $f_n$  are the eigenfunctions of  $H_o$  and  $\phi_n$  are Hermite polynomials.

Formula (9) implies that the first order correction  $\mu_1$  is real and does not depend on  $\theta$ . The same is true for all  $\mu_k$ . Indeed, it is easily seen that the parameter  $\theta$  enters the problem in a specific way. If one passes to the new variable  $t$  and proceeds with calculation of higher order corrections, all the relations thus obtained do not contain any complex values except for  $t$  as an integration variable. Thus, one only deals with integrals of the form  $\int_{-\infty}^{\infty} p(t) dt$  which do not depend on  $\theta$  and, therefore, are real.

Using the creation–annihilation technique based on the corresponding decomposition of the operator  $H_o$  (see the previous section), we calculate the first order correction for the  $n$ -th eigenvalue implicitly. Thus, formula (9) becomes

$$(10) \quad \mu_1 = \mu_1(n) = -\frac{3}{4}(2n^2 + 2n + 1), \quad n = 0, 1, \dots$$

Following the same numerical procedure (see Section 3) we compute some of the eigenvalues of  $H_\theta$ . These results can be found in Subsection 5.4.

**5.3. Numerical Range and Complex Resonances.** The resonances must turn away from the real axis as their absolute value increases, because of the fact that a resonance  $z$  is an eigenvalue of  $H_\theta$ . This implies that

$$z \in \bigcap_{0 < \theta < \pi/2} N(\theta)$$

where  $N(\theta)$  is the numerical range of the operator  $H_\theta$ . The numerical range of  $H_\theta$  is defined by

$$\begin{aligned} N_\theta &:= \{ \langle H_\theta f, f \rangle : \|f\| = 1 \} \\ &= \left\{ \int \{ V_\theta(x) |f(x)|^2 + e^{-i\theta} |f'(x)|^2 \} dx : \|f\| = 1 \right\} \\ &\subseteq \left\{ \int V_\theta(x) |f(x)|^2 dx : \|f\| = 1 \right\} + e^{-i\theta} [0, \infty) \\ &\subseteq \text{conv} \{ V_\theta(x) : x \in R \} + e^{-i\theta} [0, \infty), \end{aligned}$$

where

$$V_\theta(x) := e^{i\theta} x^2 e^{-e^{i\theta} x^2 / b^2}.$$

For small positive  $\theta$  the set  $N(\theta)$  crosses the real axis near  $x \sim 0.461b^2$ .

Indeed, if we represent  $V_\theta(x) = X_\theta(x) + Y_\theta(x)$  and denote the point where  $N(\theta)$  meets the real axis by  $(B_\theta, 0)$  then a simple calculation gives us

$$B_\theta = X_\theta + Y_\theta \cot \theta = b^2 \max \{ x^2 e^{-x^2} (2 - x^2) : x \in R \} + O(\theta) = 0.461b^2 + O(\theta).$$

Therefore the imaginary parts of any resonances must start decreasing before their real parts reach this value. This is in good accordance with the numerical data quoted in the next subsection.

**5.4. Numerical Results.** Lower eigenvalues of the operator  $H_\theta$  lying close to the real axis for different values of  $\nu$  are given in Tables 6, 7. The computed eigenvalues proved not to depend on  $\theta$ , so our numerical results are in agreement with the theoretical arguments of Section 5.1. The fact that for a range of  $\theta$  lower eigenvalues coincide up to a high accuracy shows the stability of our method as a whole.

Remark that the results to be reported below are consistent with formulae (9) and (10); they confirm, in particular, that  $\mu_1 < 0$ . On the other hand, these results illustrate the fact that series (8) is asymptotic rather than convergent. This only implies that the imaginary parts of the resonances have to be very small within the regime for which the asymptotic expansion provides useful information.

Table 6. Resonances of  $H_0$ ,  $n = 0, 1$

$\nu$	$\lambda_0$	$\lambda_1$
0.	1.	3.
$10^{-4}$	0.999925	2.999677
$4 \cdot 10^{-4}$	0.999700	2.998502
$10^{-3}$	0.999251	2.996253
$10^{-2}$	0.992475	2.962115
0.04	0.969405	2.824312
0.1	$0.920295 - 2 \cdot 10^{-6}i$	$2.560861 - 0.003347i$
0.2	$0.822647 - 0.005282i$	$2.028250 - 0.249944i$
0.25	$0.768023 - 0.019417i$	$1.850388 - 0.425748i$

Table 7. Resonances of  $H_0$ ,  $\nu = 10^{-4}$

$n$	$\lambda_n$	$n$	$\lambda_n$
0	0.999925	18	36.948571
1	2.999677	20	40.936844
2	4.999025	22	44.923925
3	6.998125	24	48.909797
4	8.996924	26	52.894462
5	10.995877	28	56.877922
6	12.993623	30	60.860175
7	14.991344	40	80.753321
8	16.989119	50	100.616298
9	18.986242	60	120.449097
10	20.983418	70	140.237430
12	24.976502	80	160.000434
14	28.968399	90	179.874965
16	32.959086	100	199.664121

Along with Table 7 we present some plots (see Figures 1a–1c). They include contour maps of the function  $F(z; a)$  defined in Section 3 whose zeros are the eigenvalues we are looking for. One can see that the zeros and the poles of  $F$  interchange (we have plotted  $F$  for Neumann boundary condition at  $x = 0$ , i.e., its zeros are the even eigenvalues, while the poles correspond to the odd ones). For  $|z| \leq 200$  we have discovered 100 eigenvalues all being real up to the accuracy  $\delta = 10^{-6}$ . Note that for different values of  $a$  (an intermediate matching point) we obviously get quite different functions  $F(z; a)$  (compare Figure 1a to 1c) while their zeros remain the same.

Given a certain number  $n$  we watch  $\lambda_n$  changing as  $\nu$  increases and compare this eigenvalue with its first order approximation (see (8)).

Table 8. Eigenvalues of  $H_\theta$ ,  $n = 10, 30$

$\nu$	$\lambda_{10}$	$\lambda_{10}^{(o)} + \mu_1(10)\nu$	$\lambda_{30}$	$\lambda_{30}^{(o)} + \mu_1(30)\nu$
$10^{-4}$	20.9834	20.9834	60.8602	60.8604
$10^{-3}$	20.8332	20.8343	59.5781	59.6043
$2 \cdot 10^{-3}$	20.6643	20.6685	58.0976	58.2085
$4 \cdot 10^{-3}$	20.3195	20.3370	54.9090	55.4170
$6 \cdot 10^{-3}$	19.9644	20.0005	51.2492	52.6255
$8 \cdot 10^{-3}$	19.5531	19.6740	$46.2597 - 0.1492i$	49.8340
$9 \cdot 10^{-3}$	19.3747	19.5083	$43.3597 - 1.5496i$	48.4383
$10^{-2}$	19.2045	19.3425	$41.2601 - 3.2488i$	47.0425

It is seen from Table 8 that only for a narrow range of  $\nu$  do the perturbation theory formulae (8) approximate actual eigenvalues (compare to Table 6). As  $\nu$  increases a typical eigenvalue deviates gradually from the value given by (8) and at some stage its imaginary part becomes substantial.

The values of the instability indices of resonances depend on  $\theta$ , even though the positions of the resonances do not. We have observed that the indices are in fact monotonically increasing functions of  $\theta$ . While this is not surprising we have no proof of the fact. We have also observed that the instability indices are increasing functions of  $b$ , provided one follows the ‘same’ resonance as  $b$  increases. The instability indices  $\kappa_n$ ,  $n = 0, 10, 20$ , computed for a wide range of  $\theta$  and  $b$  are given in the following three tables.

Table 9.1. Instability indices  $\kappa_n$ ,  $n = 0$ 

$\nu \setminus \theta$	$\pi/30$	$\pi/8$	$\pi/6$	$\pi/4$	$\pi/3$	$\pi/2.5$
0.	1.002750	1.040381	1.074570	1.189207	1.414214	1.798908
$10^{-4}$	1.002750	1.040378	1.074563	1.189185	1.414134	1.798588
$10^{-2}$	1.002729	1.040039	1.073886	1.186951	1.406329	1.769120

Table 9.2. Instability indices  $\kappa_n$ ,  $n = 10$ 

$\nu \setminus \theta$	$\pi/3000$	$\pi/300$	$\pi/30$	$\pi/20$	$\pi/10$
0.	1.000028	1.0233	1.3299	1.8249	6.6784
$10^{-4}$	1.000027	1.0209	1.3294	1.8243	6.6728
$10^{-2}$	1.000031	1.0028	1.3046	1.7562	5.9928
$\nu \setminus \theta$	$\pi/8$	$\pi/6$	$\pi/5$	$\pi/4$	$\pi/3$
0.	14.2777	57.4539	195.9499	1565.2614	$1.3645551 \cdot 10^5$
$10^{-4}$	14.2836	57.3505	195.4619	1558.9429	$1.3507237 \cdot 10^5$
$10^{-2}$	12.3306	45.7594	143.8155	965.0957	$4.6122845 \cdot 10^4$

Table 9.3. Instability indices  $\kappa_n$ ,  $n = 20$ 

$\nu \setminus \theta$	$\pi/20$	$\pi/10$	$\pi/6$	$\pi/5$	$\pi/4$	$\pi/3$
0.	5.9275	113.5766	9850.7214	$1.1753 \cdot 10^5$	$7.4538 \cdot 10^6$	$3.6609 \cdot 10^{10}$
$10^{-4}$	5.9190	113.1898	9782.2812	$1.1641 \cdot 10^5$	$7.3412 \cdot 10^6$	$3.6119 \cdot 10^{10}$
$10^{-3}$	5.6055	109.2017	9128.5324	$1.0610 \cdot 10^5$	$6.3605 \cdot 10^6$	$3.4647 \cdot 10^{10}$
$10^{-2}$	4.7349	75.0929	4811.8348	$4.5459 \cdot 10^4$	$1.6894 \cdot 10^6$	$1.7152 \cdot 10^9$

Finally, let us cite some results obtained for  $b = 10$ . In this case we have found numerically several resonances, which are real up to the chosen accuracy  $\delta = 10^{-4}$ , and a series of complex ones. As is seen, starting from about  $n = 20$  their imaginary part rapidly increases in absolute value. In fact, for different values of  $\theta$  the number of resonances with negative imaginary parts varies. The resonances and the relevant instability indices are tabulated below. In Table 10 we cite the eigenvalues  $\lambda_n$  of  $H_\theta$  along with the corresponding instability indices  $\kappa_n$  calculated for  $\theta = \pi/4$  and  $\theta = \pi/16$ .

The data of Table 10 is illustrated by the plot of  $F(z)$  (Figure 2a) and its contour

maps (Figures 2b, 2c). Remark that the largest instability indices for  $\theta = \pi/4$  and  $\theta = \pi/16$  correspond to the 26-th and the 24-th eigenvalue respectively (here we have concentrated on even eigenvalues; odd eigenvalues behave similarly). Figures 2b, 2c also show that the most unstable eigenvalues are related to  $n = 24$  and  $n = 26$ . They appear to be the first eigenvalues with negative imaginary parts — as one can see, the following eigenvalues go to the complex plane quite abruptly. We do not have any theoretical explanation of this fact except for the remark on the boundedness of  $\kappa_n$  made in the end of Section 4. Anyway, the contour maps and the values of  $\kappa_n$  agree very well and imply the same — the maximum of  $\kappa_n$  is obtained for the ‘critical’ range of the spectral parameter where eigenvalues start moving away from the real axis.

Note that though for  $\theta = \pi/16$  and  $\theta = \pi/4$  the contour map plots are quite similar, this only means that the first 28 eigenvalues coincide for the two operators. As we know, there are no eigenvalues of  $H_\theta$  below the line  $e^{-i\theta} \times [0, \infty)$ . The spots indicating the zeros of the function  $F(z)$  which are beyond the range  $\{z : -\theta < \arg z \leq 0\}$  correspond to solutions of  $H_\theta f = zf$  growing at infinity rather than decaying. Thus, in the considered example we should only regard the first 28 zeros as the eigenvalues of  $H_\theta$ ,  $\theta = \pi/16$ . They coincide with those obtained for  $\theta = \pi/4$  as we expected. We believe that our results are reliable because of their stability under the variation of several parameters involved in the problem.

Table 10. Values of  $\lambda_n$  and  $\kappa_n$  for  $\nu = 10^{-2}$

$n$	$\lambda_n$	$\kappa_n, \theta = \pi/4$	$\kappa_n, \theta = \pi/16$
0	0.9925	1.1870	1.0097
2	4.9009	2.8983	1.0684
4	8.6836	11.3609	1.2100
6	12.3350	49.4772	1.4462
8	15.8488	219.4180	1.7974
10	19.2174	960.5058	2.2918
12	22.4312	4075.82	2.9652
14	25.4782	$1.6515 \cdot 10^4$	3.8576
16	28.3422	$6.2860 \cdot 10^4$	5.0033
18	31.0004	$2.1989 \cdot 10^5$	6.4039
20	$33.7512 - 0.0003i$	$1.3978 \cdot 10^6$	9.5706
22	$35.5098 - 0.0014i$	$1.5650 \cdot 10^6$	10.0018
24	$37.0693 - 0.1593i$	$2.4535 \cdot 10^6$	10.2337
26	$38.7468 - 1.0004i$	$2.8963 \cdot 10^6$	8.8755
28	$39.8045 - 2.0367i$	$2.5627 \cdot 10^6$	7.0743
30	$41.2601 - 3.2488i$	$1.8339 \cdot 10^6$	
32	$42.6021 - 4.7565i$	$1.3337 \cdot 10^6$	
34	$45.6102 - 8.0230i$	$4.2730 \cdot 10^5$	
36	$47.0034 - 9.8515i$	$2.3134 \cdot 10^5$	

## 6. CONCLUSIONS

The instability index of an eigenvalue of a non-self-adjoint ordinary differential operator was defined in Section 2, where we investigated its theoretical properties. We have described a known general numerical procedure for computing the eigenvalues of the differential operator and have introduced a new and numerically stable procedure for computing the instability indices.

In order to test this procedure, we have carried out extensive computations for the harmonic oscillator with a complex coefficient. The eigenvalues  $\lambda_n$  of this operator are given by an exact formula, and we found close agreement between the formula and our numerical results for  $n \leq 100$ . We have also computed the instability index by two independent methods, the first being the general procedure mentioned above. The second uses a special numerical technique only available for the harmonic operator, but capable of yielding extreme accuracy if implemented in Maple with high precision arithmetic. The instability indices of the first 40 eigenvalues obtained by the two methods were found to be in close agreement; see

Table 4.

The discrepancies between the two methods are partly explained by the very high values of the instability indices of the eigenvalues  $\lambda_n$  for  $n \geq 40$ . This phenomenon was first observed for the harmonic oscillator in [9, 10] where we approached the phenomenon via pseudospectral theory. Our current approach has the advantage that it provides a quantitative measure of the instability of individual eigenvalues under small perturbations of the potential. We have carried out numerical experiments and confirmed that the size of the effects predicted matches what we have observed for a particular perturbation. In Section 4 we have conjectured on the basis of the numerical results that the eigenfunctions of the complex harmonic oscillator do not form a conditional basis.

We have also investigated the complex resonances of a typical self-adjoint operator by means of the standard technique of dilation analyticity. This identifies the resonances of the original operator with eigenvalues of any one of a family of associated non-self-adjoint operators indexed by an angle. The eigenvalues of these operators are independent of the angle, but the instability indices depend upon its value.

We have discovered that for a certain operator, as is seen from Table 10, the first 20 eigenvalues have very small imaginary parts, which is explained by the fact that there exists a (non-convergent) asymptotic expansion which has real coefficients of all orders. For higher eigenvalues the imaginary parts of the eigenvalues increase rapidly in absolute value. We have computed the instability indices of these eigenvalues for typical angles and discovered that they increased rapidly with the modulus of the eigenvalue, reaching a maximum value near the region where the imaginary part starts to increase (see Tables 9.1–9.3, 10). No theoretical explanation of this phenomenon exists.

The very large size of the instability indices in both examples indicates that the computation of large eigenvalues of non-self-adjoint differential operators is likely to be intrinsically intractable in many other cases of a similar type. The same applies to the computation of large resonances of self-adjoint differential operators. The effect of rounding errors or of small perturbations of the operator may be to change the computed eigenvalues drastically. This discovery casts some doubt on the significance of theoretical investigations of the asymptotic distributions of resonances or of any computations of such eigenvalues for all except self-adjoint operators. Our experience, and that of others who work within the pseudospectral approach, has been that the extreme instability of large eigenvalues is the norm rather than a possibility which occurs only in pathological cases.

**Acknowledgments** The authors are grateful to Prof. A. A. Abramov, who first suggested this approach to the investigation of instabilities, for useful discussions of different aspects of the paper.

## REFERENCES

1. A. A. Abramov, Zh. vychisl. Mat. mat. Fiz. **1**, (1961) 542–545 (Russian).
2. A. A. Abramov, K. Balla and N. B. Konyukhova, Comput. Math. Banach Center Pubs **13**, (1984) 319–351.
3. Abramov A.A. and Yukhno L.F. Comp. Maths Math. Phys. **34**, (1994) 671–677.
4. N. S. Bakhvalov, *Numerical Methods*, (Nauka, Moscow 1973) (Russian).
5. A. Böttcher, J. Int. Eqns Appl. **6**, (1994) 267–301.
6. A. Böttcher, *Lectures on Operator Theory and its Applications* (Fields Institute Monographs, ed. Peter Lancaster. Amer. Math. Soc. Publ., Providence, RI 1995) 2–74.
7. H. L. Cycon, R. G. Froese, W. Kirsch and B. Simon, *Schrödinger Operators; With Application to Quantum Mechanics and Global Geometry* (Texts and Monographs in Physics, Springer–Verlag, Berlin 1987).
8. E. B. Davies *Pseudospectra of differential operators* (Preprint, King’s College London, UK 1997).
9. E. B. Davies, Proc. Roy. Soc. London A **454**, (1998) to appear.
10. E. B. Davies, Commun. Math. Phys., to appear.
11. S. K. Godunov, Uspekhi Mat. Nauk **16**, 3 (99) (1961) 171–174 (Russian).
12. I. C. Gohberg and M. G. Krein, Transl. Amer. Math. Soc. **18**, (1969) 309–316.
13. P. D. Hislop and I. M. Sigal *Introduction to Spectral Theory* (Springer–Verlag, New York 1966).
14. T. Kato, *Perturbation Theory of Linear Operators* (Springer, Berlin 1966).
15. S. C. Reddy, J. Int. Eqns Appl. **5**, (1993) 369–403.
16. S. C. Reddy and L. N. Trefethen, SIAM J. Appl. Math. **54**, (1994) 1634–1649.
17. L. Reichel and L. N. Trefethen, Linear Alg. Appl. **162–164**, (1992) 153–185.
18. K.-C. Toh and L. N. Trefethen, SIAM J. Sci. Comp. **17**, (1996) 1–15.
19. L. N. Trefethen, *D F Griffiths and G A Watson, Numerical Analysis 1991* (Longman Sci. Tech. Publ., Harlow, UK 1992) 234–266.
20. L. N. Trefethen, SIAM Review **39**, (1997) 383–406.

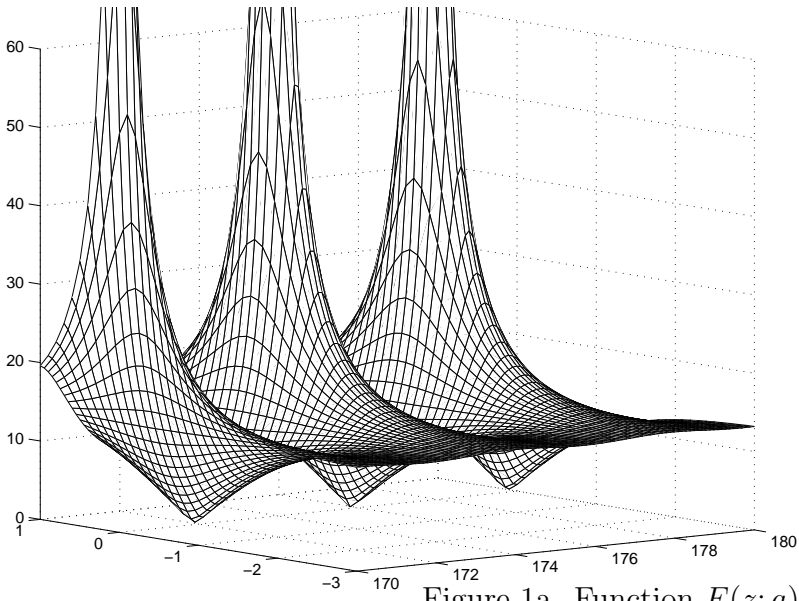
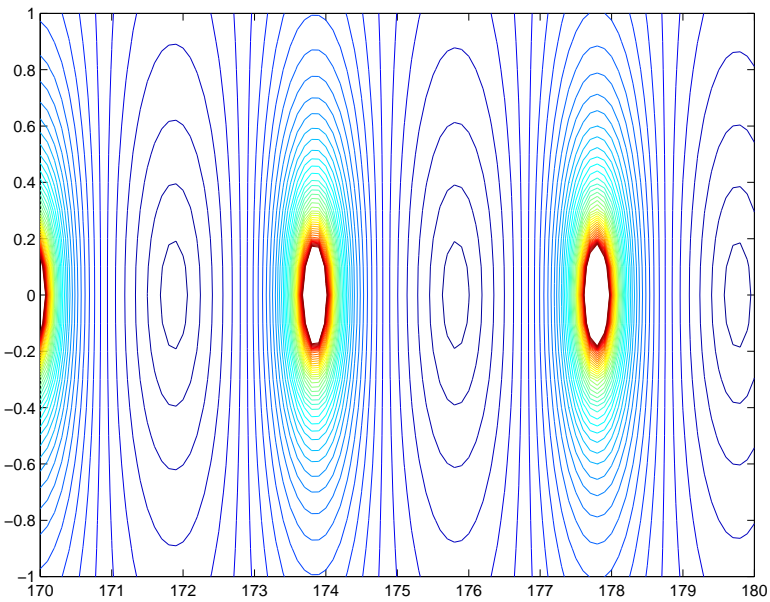
Figure 1a. Function  $F(z; a)$ ,  $a = 0$ ,  $b = 100$ Figure 1b. Contour map of  $F(z; a)$

Figure 1c. Plot and contour map of  $F(z; a)$ ,  $a = 4$ ,  $b = 100$

Figure 2a. Function  $F(z; 0)$ ,  $b = 10$ ,  $\theta = \pi/4$

Figure 2b. Contour map of  $F(z; 0)$ ,  $b = 10$ ,  $\theta = \pi/4$

Figure 2c. Contour map of  $F(z; 0)$ ,  $b = 10$ ,  $\theta = \pi/16$

DEPARTMENT OF MATHEMATICS, KING'S COLLEGE, STRAND, LONDON WC2R 2LS, UK

*E-mail address:* Aslanyan@mth.kcl.ac.uk, E.Brian.Davies@kcl.ac.uk

